ELSEVIER

Exergy Int. J. 1(3) (2001) 209–215

Exergy, an International Journal

www.exergyonline.com

Flow through a protruding bluff body–heat and irreversibility analysis

S.Z. Shuja*, B.S. Yilbas, M.O. Iqbal, M.O. Budair

Mechanical Engineering Department, King Fahd University of Petroleum and Minerals, Dhahran, Saudi Arabia

(Received 1 September 1999, accepted 19 January 2000)

Abstract — Flow over a protruding bluff body finds wide application in many engineering fields. The modeling of the conjugate heating process due to bluff body gives insight into the physical process involved and minimizes the experimental cost. In the present study, the transient conjugate heat transfer analysis of the bluff body subjected to low Reynolds number flow is considered. The governing flow and energy equations are solved numerically using a control volume approach. The heat transfer characteristics are examined through the normalized Stanton number. The entropy generation due to fluid friction and heat transfer in the fluid system is computed and ratio of rate of heat transfer to irreversibility generated is obtained. It is found that the heat transfer in the region of top and bottom edges of the bluff body is enhanced due to the convection effect. The heat transfer to irreversibility ratio decreases sharply as the heating progresses. © 2001 Éditions scientifiques et médicales Elsevier SAS

heat transfer / entropy / irreversibility

Nomenclature

Cp	specific heat	$\mathrm{J{\cdot}kg^{-1}{\cdot}K^{-1}}$
D	height of protruding body	m
h	heat transfer coefficient	$\mathrm{W{\cdot}m^{-2}{\cdot}K^{-1}}$
I	irreversibility	$\mathrm{W{\cdot}m^{-3}{\cdot}K^{-1}}$
Nu	Nusselt number	
q'''	heat flux	$\mathrm{W{\cdot}m^{-3}}$
Q	heat transfer per unit volume	$\mathrm{W{\cdot}m^{-3}}$
St	Stanton number	
S'''	volumetric entropy generation	$\mathrm{W{\cdot}m^{-3}{\cdot}K^{-1}}$
T	temperature	K
T_{o}	reference temperature	K
u	velocity in the x-axis	$\mathrm{m{\cdot}s^{-1}}$
v	velocity in the y-axis	$\mathrm{m{\cdot}s^{-1}}$
x	x-axis	
y	y-axis	

Greek symbols

ν	kinematic viscosity	$\mathrm{m^2{\cdot}s^{-1}}$
ρ	density	$\mathrm{kg{\cdot}m^{-3}}$
μ	dynamic viscosity	$\mathrm{N{\cdot}m{\cdot}s^{-2}}$
φ	variable	

Subscripts

f	fluid
s	solid
w	wall
∞	infinity
o	reference
gen	generation

* Correspondence and reprints.
E-mail address: shuja@kfupm.edu.sa (S.Z. Shuja).

1. INTRODUCTION

Flow past a protruding body is an attractive research topic of various disciplines in many engineering problems such as in heating and cooling systems. The body produces a wake flow in the downstream which is related with the flow mixing and; consequently, the heat transfer enhancement from the body. There is a need in practice to determine the heat transfer characteristics of such flow. The current state of computational bluff body aerodynamics was presented by Laurence and Mattei [1]. They indicated that for industrial flows, the software developed gave reliable and sufficiently detailed information for predicting mean flow and temperature fields. The comparison of large eddy simulation (LES) and Reynolds-

S1164-0235(01)00027-9/FLA

averaged Navier–Stokes (RANS) calculations of the flow around bluff bodies was carried out by Rodi [2]. He indicated that LES was more suited and has great potential for calculating these complex flows as compared to RANS. The influence of the no slip boundary condition on the numerical simulation of two-dimensional incompressible flow past a circular cylinder was investigated using a numerical code [3]. They showed that the formulation for the no-slip boundary condition on the cylinder surface had strong importance in the computation of the different characteristics parameters, but it had very little importance in the general description of the flow.

Heat transfer for an axisymmetric confined jet with a bluff body in a tube was investigated by Senda et al. [4]. They indicated that a local minimum appeared in the distribution of Nusselt number of an axisymmetric confined jet with a cylindrical ring. The collapse of vortices generated behind the bluff body increased the heat transfer coefficient. The problem of mixed convection heat and mass transfer, including internal conduction inside the cylinder in the presence of a surface reaction of arbitrary order was investigated by a Fourier-spectral element method [5]. They concluded that the temperature and concentration fields become asymmetrical about the horizontal axis and the flow separation from the cylinder surface lead to dispersed fluid particles with higher temperature gradients. A numerical investigation of laminar mixed convection from a horizontal isothermal cylinder was carried out by Chen et al. [6]. They showed that the reverse flow in the wake of the cylinder was strongly influenced by ratio of $Gr/Re2$ and increasing Gr increases Nu. The heat transfer on the surface of the five different elements was investigated by Chyu and Natarajan [7]. They indicated that the vortex structures generated for each bluff body had enhanced the heat transfer coefficient considerably. Turbulent heat transport in a boundary layer behind a junction of a streamlined cylinder and a wall was investigated by Wroblewski and Eibeck [8]. They indicated that peak values of the Stanton number and the eddy diffusivity were observed in the inner-wake region.

On the other hand, considerable research studies were conducted for the entropy analysis of the thermal system. The entropy minimization of thermal system offers optimal design and operation of that system. This is because the minimization of the irreversibilities generated due to fluid friction and heat transfer improves the second law efficiency of the system. The control volume method was used to establish the rate of entropy generation due to heat and mass transfer in a fluid system accompanied by fluid friction [9]. The resulting entropy rate equations were applied to examples of simultaneous heat and mass transfer in internal and external flows. The second law aspects of heat transfer by forced convection were illustrated by Bejan [10] in terms of different fundamental flow configuration. He showed that the flow geometric parameters could be selected in order to minimize the irreversibility associated with a specific convection heat transfer process. Andersen and Gordon [11] investigated the optimal paths for minimizing entropy generation in a common class of finite-time heating and cooling processes. The solutions pertained to generalized heat transfer law were illustrated quantitatively for cases of practical interest including radiative heat transfer. They indicated that the potential savings in entropy generation achievable with the optimal strategy increased as the ratio of process time to system relaxation time Increased. In addition, a comprehensive survey on the entropy generation was carried out by Bejan [12].

In the present study, flow past over the protruding rectangular bluff body is considered. The two-dimensional governing equations of flow field and heat transfer were computed using a control volume approach. The normalized Stanton number variation in the span wise direction of the bluff body was obtained. The entropy generation in the system is computed and the heat transfer to irreversibility ratio is determined.

2. MATHEMATICAL MODELING

Figure la shows the schematic view of the protruding square body. The flow around the protruding bluff body is assumed as incompressible and laminar since the Reynolds number considered at present is 13 in order to avoid the three-dimensional vortex shedding. The governing equations are given as follows.

The continuity equation.

$$\frac{\partial u}{\partial x} + \frac{\partial v}{\partial y} = 0 \qquad (1)$$

The momentum equation. x-momentum

$$u\frac{\partial u}{\partial x} + v\frac{\partial u}{\partial y} = -\frac{1}{\rho}\frac{\partial P}{\partial x} + \nu\left(\frac{\partial^2 u}{\partial x^2} + \frac{\partial^2 u}{\partial y^2}\right) \qquad (2)$$

y-momentum

$$u\frac{\partial v}{\partial x} + v\frac{\partial v}{\partial y} = -\frac{1}{\rho}\frac{\partial P}{\partial y} + \nu\left(\frac{\partial^2 v}{\partial x^2} + \frac{\partial^2 v}{\partial y^2}\right) \qquad (3)$$

The energy equation

$$\rho Cp\left(\frac{\partial T}{\partial t}+u\frac{\partial T}{\partial x}+v\frac{\partial T}{\partial y}\right)=k\left(\frac{\partial^2 T}{\partial x^2}+\frac{\partial^2 T}{\partial y^2}\right)+\mu\phi \tag{4}$$

where

$$\phi=2\left(\left(\frac{\partial u}{\partial x}\right)^2+\left(\frac{\partial v}{\partial y}\right)^2\right)+\left(\frac{\partial v}{\partial x}+\frac{\partial u}{\partial y}\right)^2 \tag{5}$$

The initial and boundary conditions. The initial conditions:

At time zero ($t=0$), $u=u(y)$ and $T=T_o$ in the flow field and heat input is zero ($q'''=0$).

At solid wall:

$$u=0 \text{ and } v=0 \text{ (no slip condition)}$$

At inlet and exit a uniform fluid temperature and uniform flow are assumed.

At $x=0$ and $x=1.14$ m (along x-axis) and

$$y=0 \text{ and } y=0.82 \text{ m (along } y\text{-axis)}$$

$$\frac{\partial\varphi}{\partial x}=0 \quad \text{and} \quad \frac{\partial\varphi}{\partial y}=0$$

where φ is any of the fluid property such as velocity and temperature.

Protruding solid body. Energy equation

$$\rho Cp\left(\frac{\partial T}{\partial t}\right)=k\left(\frac{\partial^2 T}{\partial x^2}+\frac{\partial^2 T}{\partial y^2}\right)+q''' \tag{6}$$

where q''' is the uniform heat flux over the body.

Initial condition. At time zero ($t=0$)

$$q'''=0 \text{ and } T(x,y)=T_o$$

Boundary conditions. At the solid wall

$$-k\frac{\partial T}{\partial n}=h(T_w-T_o)$$

$$T_s=T_f \quad \text{and} \quad q'''=1.25\times10^5\ \text{W·m}^{-3}$$

The selection of q''' as 1.25×10^5 W·m^{-3} is due to the comparison of entropy generation due to heat transfer and fluid friction, i.e., high heat flux results in excessive entropy generation due to heat transfer.

The dimensionless numbers. The Stanton number:

$$St=q_w/\left[\rho CpU_\infty\sim(T_w-T_\infty)\right].$$

The normalized Stanton number: St/St_o where St_o is the maximum value in span wise direction.

The Nusselt number: $Nu=hD/k$
where

$$h=\frac{(-k\partial T/\partial n)_{\text{wall}}}{(T_w-T_\infty)}$$

where n is the direction normal to the surface.

Entropy analysis. The volumetric rate of entropy generation is

$$S'''_{\text{gen}}=2\frac{k}{T^2}\left(\left(\frac{\partial T}{\partial x}\right)^2+\left(\frac{\partial T}{\partial y}\right)^2\right)+\frac{\mu}{T}\left(\left(\left(\frac{\partial u}{\partial x}\right)^2+\left(\frac{\partial v}{\partial y}\right)^2\right)+\left(\frac{\partial v}{\partial x}+\frac{\partial u}{\partial y}\right)^2\right) \tag{7}$$

where the first term is entropy generation due to heat transfer and the second term is due to fluid friction.

Irreversibility can be written as.

$$I=\int T_o S'''_{\text{gen}}\,\mathrm{d}\varphi \tag{8}$$

The ratio of heat transfer to irreversibility can be written as Q/I.

RESULTS AND DISCUSSION

The flow field is overlaid with a rectangular grid as shown in *figure 1(b)*, whose intersection points denote the location at which all variables except velocities are calculated. The velocities are calculated midway locations between the points. The grid independence tests are conducted, the grid size of 10800 (90 × 120) is selected, which in turn gives the grid independent results. The control volume approach is introduced when solving the governing equations numerically. A staggered grid arrangement is used. This provides the handling the pressure linkages through continuity equation, which is known as SIMPLE algorithm. The steady state convergence is achieved by successively predicting and correcting the velocity components and the pressure.

Figure 2 shows the velocity contours. The velocity contours extends in downstream of the flow, which in turn

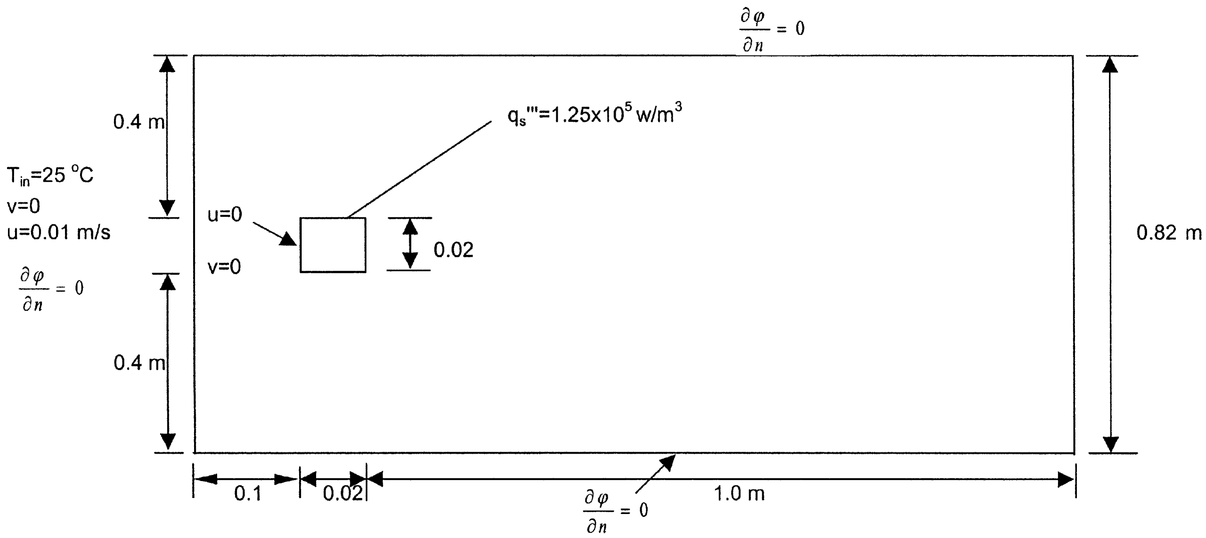

(a)

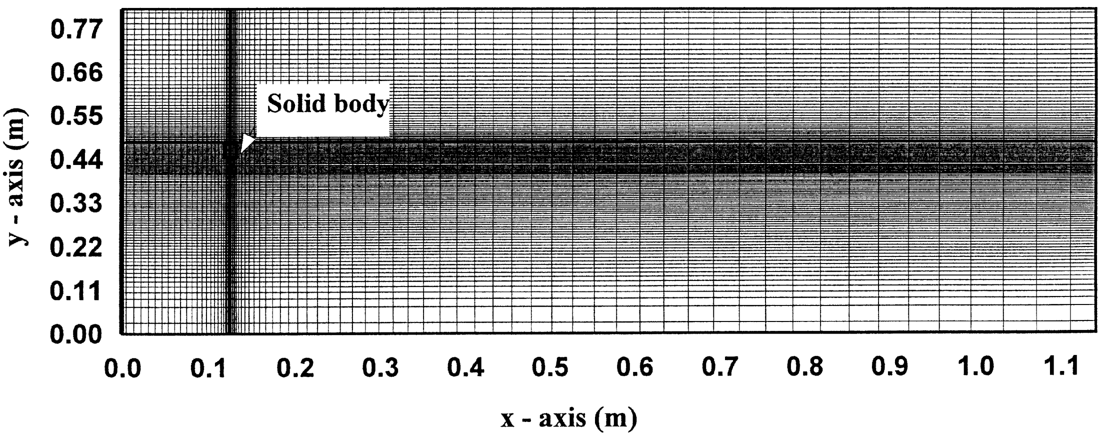

(b)

Figure 1. (a) Schematic view of the block and boundary conditions. (b) Mesh used in the computations.

generates a large wake behind the body. No circulation region is observed in the downstream of the flow. This is because the flow generates almost a creeping motion behind the body. The flow accelerates along the top and bottom surfaces of the body. This is due to the pressure drop in these regions; in this case the kinetic energy of the fluid increases. The stagnation region in front of the body extends slightly inside of the upstream flow. This is again because of the creeping motion behavior of the fluid in front of the body.

Figure 3 shows the temperature contours in the fluid. The temperature contours extend considerably in the downstream of the flow as similar to those corresponding for the velocity contours. In general, temperature field

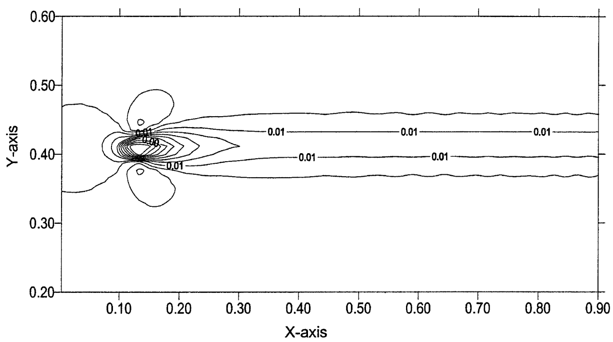

Figure 2. Velocity contours in the flow field.

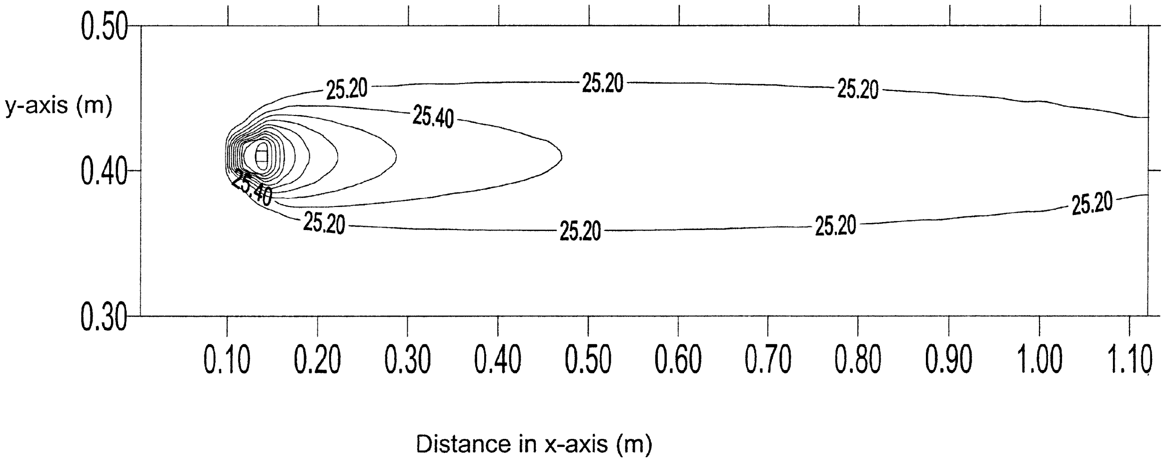

Figure 3. Temperature contours in the flow field.

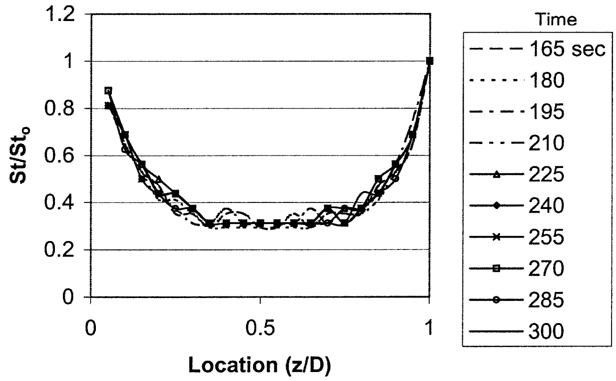

Figure 4. Normalized Stanton number (St/St_0) with dimensionless distance along the span wise direction as variable is time.

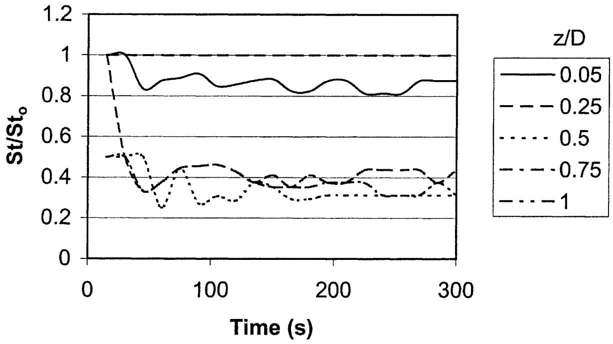

Figure 5. Normalized Stanton number (St/St_0) with time as variable is z/D.

is similar to the velocity field in the downstream of the flow. However, they differ in the vicinity of the surface. In this case, temperature contours close to the rear side of the body attain higher values than the temperature contours in further downstream of the wake. The cooling in this region is not substantial due to the less significant convection effect, i.e., the fluid velocity in this region is not sufficiently high to substantiate the convection cooling.

Figure 4 shows the normalized Stanton number (St/St_0) in the span-wise direction of the rear side of the bluff body, while *figure 5* shows the time variation of the normalized Stanton number (St/St_0). Normalized Stanton number attains the lowest values in the central region of the rear surface in the span wise direction. This occurs because less convection cooling of the surface is resulted in this region. Alternatively, as the distance from the center of the body in the span wise direction increases, St/St_0 increases to reach maximum at the edges of the body. This is because of the fact that the convection acceleration close to top and bottom surfaces of the body is high due to the pressure drop in this region. This accelerates the flow in the region close to the edges of the rear side of the body. Consequently, the convection cooling enhances in these regions because of the fluid motion St/St_0 variation with time shows the small oscillation. This indicates the small boundary layer separation in this region. Since the oscillation is resulted almost at all locations in the span wise direction, except at the center of the body, the boundary layer separation extends almost over the whole region of the rear side of the body. However, the transient behavior of St/St_0 is only observed in the early heating times.

Figure 6 shows the constant entropy contours around the body and includes the entropy generation due to fric-

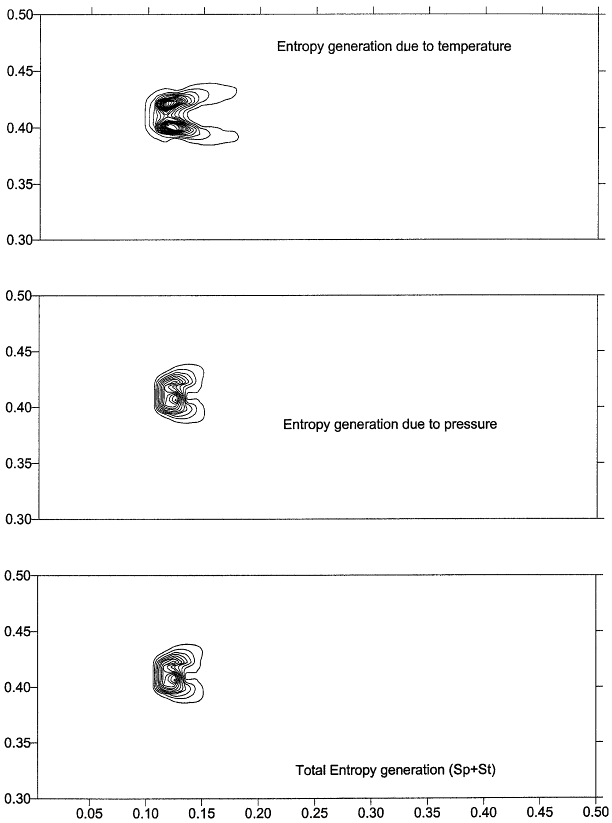

Figure 6. Entropy contours around a bluff body.

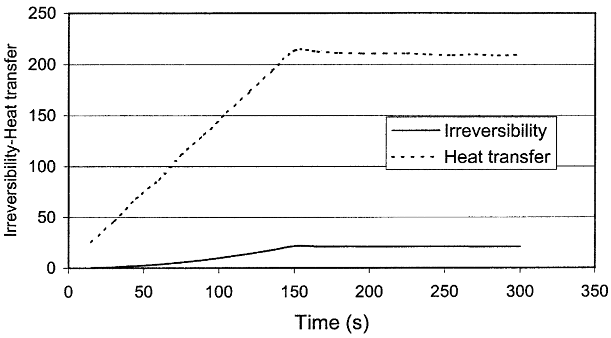

Figure 7. Irreversibility and heat transfer with time.

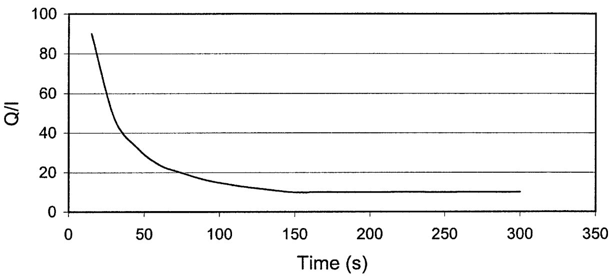

Figure 8. Heat transfer to irreversibility ratio with time.

tional and heat transfer contributions. The entropy contours are densely populated around the body especially for the fluid friction contribution. This is due to the viscous dissipation, which is considerably high around the body. The entropy generation due to heat transfer extends inside the downstream of the flow. This is because of the temperature gradient developed in the flow, i.e., the convection enhances the heat transfer and extends the temperature field further downstream of the flow. When comparing the entropy generation due to fluid friction and heat transfer, it can be observed from *figure 7(c)* that the entropy generated due to fluid friction dominates the total entropy generation in the system.

Figure 7 shows the temporal variation of irreversibility generated in the system due to fluid flow and heat transfer. The irreversibility increases gradually as the heating progresses. However, it reaches a steady value after the heating of about 150 s. The increase in irreversibility during the early heating period is due to heat transfer contribution of the entropy generation, i.e., the entropy generation increases as the temperature gradient in the fluid increases. This occurs only in the early heating period. Therefore, once the heating progresses, the heat transfer from the body to the fluid reaches to a steady value. In this case, the entropy generation remains almost the same during the steady heating cycle.

Figure 8 shows the temporal variation of the ratio of heat transfer to the irreversibility generated in the system (Q/I). The Q/I attains considerably high values during early heating period. This is because of the fact that the irreversibility generated and the heat transfer are less in the early time period. However, the amount of heat transfer well exceeds the irreversibility generated during this period. Consequently, their ratio becomes high. The transient period of the fluid heating by the solid body is more pronounced in the early heating period. As the heating progresses, Q/I reduces and attains a steady value. In this case, the temperature gradient in the flow field remains almost the same, which in turn results in the constant rate of entropy generation as indicated earlier.

3. CONCLUSIONS

The conclusions derived from the present work may be listed as follows:

1. The creeping motion of the flow generates almost a steady wake behind the bluff body. The acceleration

of the fluid at the top and bottom surfaces of the body is due to pressure suspension in these regions. However, no separation and reverse flow is observed from the flow field.

2. Temperature field shows the similar behavior as the flow field. The temperature gradient in the span wise direction of the rear side of the body is low which in turn indicates the low rate of cooling in this region.

3. The normalized Stanton number (St/St_0) is large at the edges of the rear surface and it decays considerably as the distance in the span wise direction increases towards the center of the body. In this case, the fluid acceleration due to low pressure gradient at the top and bottom surfaces of the body enhances the heat transfer in these region. The temporal behavior of the St/St_0 indicates the existence of periodic boundary detachment from the rear surface of the body. However, the influence of the detachment on the heat transfer characteristics is not substantial, since the amplitude of St/St_0 oscillation is very small.

4. The irreversibility generated in the system due to heat transfer and fluid friction is considerable in the early heating period. As the heating progresses, the irreversibility becomes almost steady with time, in which case, the rate of entropy generation due to temperature gradient reaches to almost a constant rate.

5. The heat transfer to irreversibility ratio (Q/I) decreases rapidly as the heating progresses. Although the heat transfer rate and irreversibility generated are small during the early heating period, the amount of heat transfer well exceeds the amount of irreversibility generated during this period. As the heating progresses Q/I attains almost a steady value. In this case, the temperature gradient in the fluid settles and its time variation becomes negligible, i.e., the ratio of heat transfer to irreversibility becomes almost constant.

Acknowledgement

The authors acknowledge the support of King Fahd University of Petroleum and Minerals, Dhahran, Saudi Arabia for this work.

REFERENCES

[1] Laurence D., Mattei J.O., Current state of computational bluff body aerodynamics, J. Wind Engrg. Inst. Aerodynamics 49 (1993) 23–44.

[2] Rodi W., Comparison of LES and RANS calculations of the flow around bluff bodies, J. Wind Engrg. Inst. Aerodynamics 69–71 (1997) 55–75.

[3] Magumder S., Rodi W., Zhu J., Three-dimensional finite-volume method for incompressible flows with complex boundaries, ASME. J. Fluids Engrg. 114 (1992) 496–503.

[4] Senda M., Kikkawa S., Odak, Okamoto S., Funabiki T., Heat transfer for an axisymmetric confined jet with a bluff body in a tube, Heat Transfer-Japanese Res. 21 (1992) 809–822.

[5] Nguyen H.D., Paik S., Douglas R.W., Convective transport about cylinder with surface reaction of arbitrary order, AlCHE. J. 42 (1996) 1514–1524.

[6] Chen C., Yang Y., Wu S., Laminar mixed convection from a circular cylinder using a body-fitted coordinate system, J. Thermophysics Heat Transfer 8 (1994) 695–701.

[7] Chyu M.K., Natarajan V., Heat transfer on the base surface of three-dimensional protruding elements, Internat. J. Heat Mass Transfer 39 (1996) 2925–2935.

[8] Wroblewski D.E., Eibeck P.A., Turbulent heat transport in a boundary layer behind a junction ofa streamlined cylinder and a wall, ASME. J. Heat Transfer 114 (1992) 840–849.

[9] Carrington C.G., Sun Z.F., Second law analysis of combined heat and mass transport in internal and external flows, Internat. J. Heat Fluid Flow 13 (1992) 65–70.

[10] Bejan A., A study of entropy generation in fundamental convective heat transfer, ASME J. Heat Transfer 101 (1979) 718–725.

[11] Anderson B., Gordon J.M., Optimal paths for minimizing entropy generation in a common class of finite-time heating and cooling processes, Internat. J. Heat Fluid Flow 13 (1992) 294–299.

[12] Bejan A., Entropy minimization: the new thermodynamics of finite-size devices and finite-time processes, J. Appl. Phys. 79 (1996) 1191–1218.